

THE EFFECT OF INLET VELOCITY ON THE PERFORMANCE OF OIL SHALE ASH CYCLONE SEPARATOR

JING-XUAN YANG^{(a)*}, GUO-GANG SUN^{(b)*},
YU-MING ZHANG^(b,c), QIANG MA^(d), CHUAN LI^(e)

- (a) College of Chemistry and Chemical Engineering, Taiyuan University of Technology, Taiyuan, 030024, China
- (b) State Key Laboratory of Heavy Oil Processing, China University of Petroleum, Beijing, 102249, China
- (c) Beijing Key Laboratory of Process Fluid Filtration and Separation, Beijing, 102249, China
- (d) Science and Technology Development Department, China National Offshore Oil Corporation, Beijing, 100027, China
- (e) Birmingham Centre for Energy Storage, University of Birmingham, Birmingham, B15 2TT, UK

Abstract: *The maximum efficiency inlet velocity (MEIV) of the oil shale ash cyclone separator was explored in this paper. The results show that the inlet area of the separator has a significant effect on MEIV. Further analysis revealed that the cross-sectional mean axial velocity for the gas in the cylinder affording the highest efficiency was hardly affected by inlet dimensions, which circumstance could be made use of in designing the cyclone diameter. Based on the results obtained, an equation was constructed and the maximum efficiency inlet velocity for oil shale ash was predicted. Moreover, the effect of particle geometry on MEIV was ascertained.*

Keywords: *cyclone separator, oil shale ash, separation efficiency, inlet velocity.*

1. Introduction

Oil shale is primarily used to produce shale oil and generate electricity by burning, during which almost 60–80% of raw oil shale is converted to a by-product, oil shale ash [1–3]. Most of the toxic elements contained in oil shale are retained in oil shale ash, which will cause serious environmental problems unless efficiently retrieved [4]. Cyclone separator is a kind of dedusting device and is widely used for ash extraction during oil shale

* Corresponding author: email ggsunbj@163.com, tyyangjingxuan@163.com

processing [4–8]. It is reported that about 33% of oil shale ash from the oil shale burning process is collected by the cyclone separator [4]. The rest of the ash is retrieved by an electric precipitator or baghouse filter in order to ensure compliance with prescribed air emission standards.

However, little research has been done on the performance of the oil shale ash cyclone separator so far. Wang et al. [9] and Wang et al. [10] investigated the separation performance of the fine oil shale ash cyclone at normal temperature. The researchers showed that the maximum efficiency inlet velocity (MEIV) was 15 m/s. When the inlet velocity of the cyclone was lower than MEIV, the separation efficiency increased with its increase. On the other hand, when the inlet velocity exceeded MEIV, the separation efficiency decreased with increasing inlet velocity. Obviously, to ensure the high efficiency of operation, the inlet velocity of the cyclone should be close to MEIV.

Previous works have reported cyclone dimensions to have an influence on MEIV. The MEIV obtained by Wang et al. [9] and Wang et al. [10] is therefore not appropriate for all types of oil shale ash cyclones. Kalen and Zenz [11] and Shi and Wu [12] proposed methods to predict the MEIV of the oil shale ash cyclone. Both the methods were used by investigators [9, 10] to predict the MEIV of experimental oil shale ash cyclones and the obtained MEIV values were respectively 11.0 and 9.7 m/s, which are both lower than 15 m/s. The calculated MEIV values were too conservative to obtain maximum separation efficiency. Moreover, Shepherd and Lapple [13] proposed the range of practicable cyclone inlet velocity to be $15 \leq v_{in} \leq 30$. However, it was still difficult to apply this principle to optimizing the inlet velocity as it was unclear which cyclone dimensions and which characteristics of oil shale particle and gas would allow this.

In short, the data obtained in earlier investigations on the MEIV of the cyclone for oil shale ash are not sufficient for its optimization. This has hampered the optimum designing of the cyclone and its use in oil shale retorting and burning devices. In this paper, an attempt has been made to determine an optimum MEIV of the oil shale ash cyclone. The results are expected to provide relevant guidance for the optimum designing and efficient use of the cyclone in the oil shale industry.

2. Experimental

The experimental apparatus used in this work is shown in Figure 1. During the tests, the oil shale ash was sucked into the cyclone by a fan blower installed at the end of the system. The particles separated from the gas were collected in the hopper underneath and then weighted to measure the separation efficiency. During each test, a fixed quantity of oil shale powder was fed to the cyclone. The dust feeding time was controlled to keep the solid loading in the air constant. The Pitot tube (Fig. 1a) was used to measure the inlet velocity of gas.

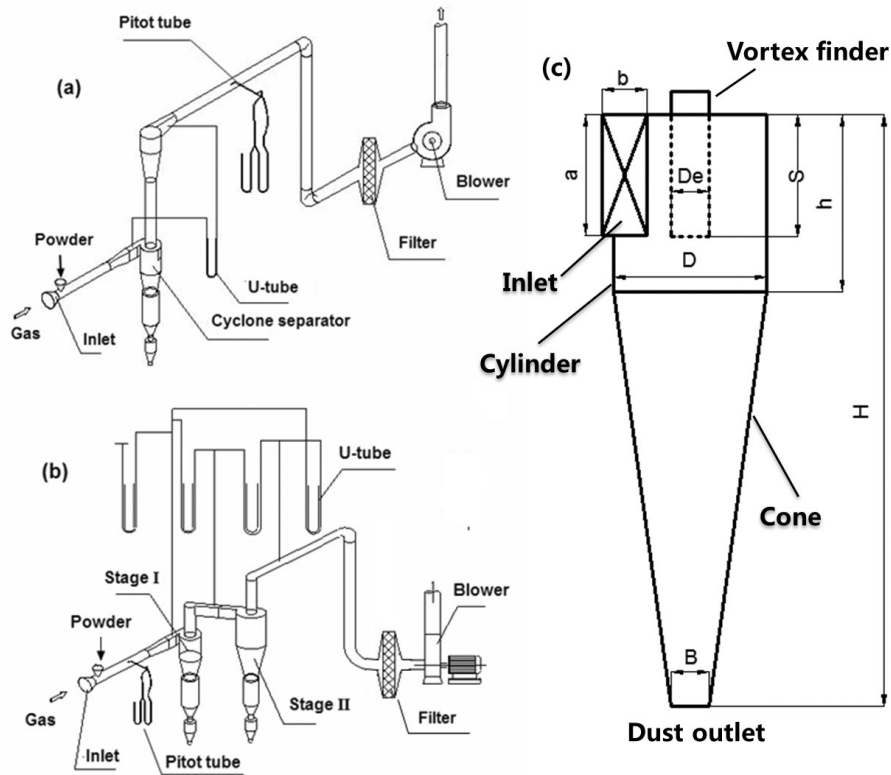


Fig. 1. Schematic illustration of experimental equipment.

The experiments were carried out using single (Fig. 1b) and two-stage cyclones in series (Fig. 1c), respectively. The dimensions of the cyclones are given in Table 1. Specially, the size of the rectangular inlet of the cyclone

Table 1. Dimensions and operating conditions of cyclones*

	Single cyclone					Cyclones in series					
						stage I	stage II	stage I	stage II	stage I	stage II
D, mm	300	300	300	900	900	900	900	900	900	900	900
KA	5.5	7.5	11	5.5	7.5	5.5	7.5	5.5	5.5	7.5	5.5
De/D	0.3	0.3	0.3	0.32	0.37	0.33	0.52	0.37	0.46	0.4	0.46
Solid loading, g/m ³	10	10	10	20	20	20	20	20	20	20	20
Median particle size, μm	14.69	14.69	14.69	4.45	4.45	4.45	4.45	4.45	4.45	4.45	4.45

* The geometry dimensions not indicated in Table 1 were the same for all the tested cyclones: B/D = 0.4; H/D = 3.5; h/D = 1.5; S/a = 1.

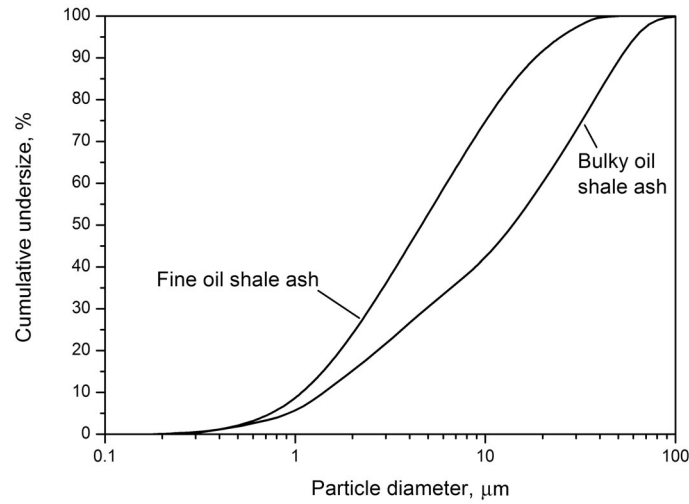


Fig. 2. Particle size distribution of test powder.

was indicated by the dimensionless parameter KA , which is the ratio of cylinder area to inlet area. Two oil shale ash samples of median particle size (14.69 and 4.45 μm , respectively) from the oil shale burning process were used as test samples. The bulk density of both samples was 1350 kg/m^3 . The particle size distribution of the tested powder samples is shown in Figure 2. The dust loads used in the tests are presented in Table 1.

3. Results and discussion

3.1. The maximum efficiency inlet velocity of oil shale ash cyclone

Figure 3 shows the effect of inlet velocity on the separation efficiency of a single cyclone. It can be observed from Figure 3a that MEIV increases with increasing KA when the cyclone diameter remains unchanged. However, when KA keeps constant, the cyclone diameter and particle size distribution have no obvious effect on MEIV. When KA was 5.5, both cyclones offered maximum efficiency at the inlet gas velocity of about 15 m/s. Similarly, the particle size distribution shows no apparent effect on MEIV.

The present theories, i.e. Equation (1) [11] and Equation (2) [12], were used to predict the MEIV of experimental oil shale ash cyclones. The results are presented in Table 2.

$$v_{MEIV} = 231.6 \left(\frac{4g\mu_g\rho_p}{3\rho_g^2} \right) \left(\frac{b/D}{1-b/D} \right) b^{0.2}. \quad (1)$$

$$v_{MEIV} = 19KA^{1.4} \left(\frac{4g\mu_g\rho_p}{3\rho_g^2} \right) \left(\frac{b/D}{1-b/D} \right) \left(\frac{b}{D} \right)^{0.2}. \quad (2)$$

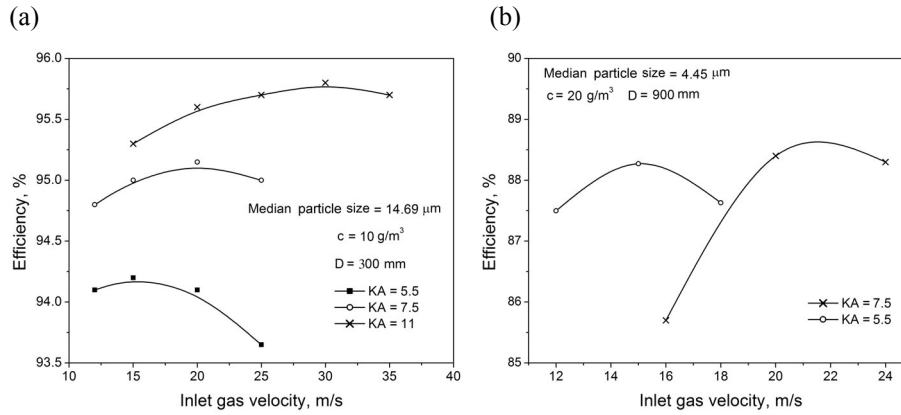


Fig. 3. The effect of inlet gas velocity on the separation efficiency of a single cyclone: (a) $D = 300$ mm, median size of test powder particle; (b) $D = 900$ mm.

Table 2. MEIV and MECMAGV of oil shale ash cyclones

D, mm	KA	Experimental MEIV, m/s	Median powder particle size, μm	Predicted MEIV, m/s			MECMAGV, m/s
				[12]	[11]	The present work	
300	5.5	15	14.69	11.1	9.8	15.4	2.73
300	7.5	20	14.69	14.1	8.0	21.6	2.67
300	11	30	14.69	18.8	6.3	32.7	2.73
900	5.5	15	4.45	11.5	12.6	15.9	2.73
900	7.5	20	4.45	14.1	10.0	21.6	2.67
Coefficient of determination				0.6783	0.3755	0.9211	–

It can be seen from Table 2 that the MEIV obtained from Equation (1) decreased with increasing KA, in contrast to the result obtained by Equation (2) and the experimental data. Moreover, the MEIV values calculated on the basis of Equations (1) and (2) were lower than the experimental data, while this discrepancy increased with the increase of KA. In the present work, a new theoretical equation on the basis of experimental data on the oil shale ash cyclone is proposed as follows:

$$v_{MEIV} = 15KA^{1.725} \left(\frac{4g\mu_g\rho_p}{3\rho_g^2} \right)^{\frac{1}{3}} \left(\frac{b/D}{1-b/D} \right) \left(\frac{b}{D} \right)^{0.2} \quad (3)$$

The MEIV values of experimental oil shale ash cyclones predicted from Equation (3) are also given in Table 2. The table reveals that the MEIV predicted from Equation (3) is much closer to the experimental data than the respective values obtained from the other equations.

3.2. The cross-sectional mean axial gas velocity in the cyclone body

The following expression can be used to calculate the cross-sectional mean axial gas velocity in the cyclone body (v_a) according to inlet velocity (v_{in}):

$$v_a = \frac{v_{in}}{KA} \quad (4)$$

Based on the experimental MEIV, the maximum efficiency cross-sectional mean axial gas velocity (MECMAGV) in the cyclone body can be obtained. Table 2 shows that the MECMAGV of all single oil shale ash cyclones under test is about 2.7 m/s, which is hardly affected by cyclone dimensions and the median size of a separated particle. Generally, the incoming dirty gas volume, Q , is constant in the oil shale processing device. If the cyclone diameter is designed according to the following expression, the cyclone separator is operated close to MEIV whatever KA is:

$$D = \sqrt{\frac{4Q}{\pi v_{MECAV}}} \quad (5)$$

During the tests on experimental cyclones in series, both D and Q in the first cyclone stage equaled those in the second stage, which ensured similar cross-sectional mean axial gas velocities in two-stage cyclones. Figure 4 shows the overall efficiency of two-stage cyclones as a function of v_a . Obviously, the maximum overall efficiency was achieved when v_a was about 2.7 m/s for all three types of two-stage cyclones. It appears that the

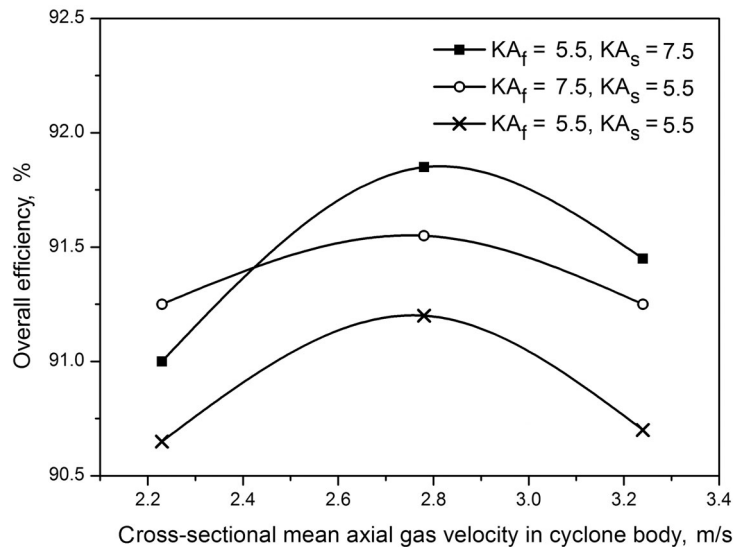


Fig. 4. The effect of cross-sectional mean axial gas velocity in the cyclone body on the overall efficiency of cyclones in series.

MECMAGV of cyclones in series equals that of the cyclone operated alone. During experiments on cyclones in series, it is necessary to calculate the MEIV of each cyclone stage based on cyclone dimensions to ensure its operation close to MEIV. However, for oil shale ash cyclones in series, this calculation will not be necessary if the diameter of each cyclone is designed according to Equation (5).

It should be noted that the MEIV of the cyclone increases when the gas viscosity is increased or the gas density decreased due to the rise in temperature. According to the relationship between MECMAGV and MEIV (Eq. (4)), the former increases with temperature. The MECMAGV values given in Table 2 were obtained at normal temperature, and are therefore not suitable for the cyclone operated at high temperature. Because there are very few reports about the MEIV of the oil shale ash cyclone, prediction of the MECMAGV of the cyclone operated at high temperature is difficult. Moreover, to our knowledge, only few studies have been carried out on the effect of solid loading on the MEIV of the cyclone. In our work, no such effect was observed at low solid loading. Thus, the results and conclusions presented in this section can be used in case of the cyclone operated at low solid loading.

3.3. The effect of particle geometry on maximum efficiency inlet velocity

In a previous work, Wang et al. [10] have reported the separation efficiency of a single cyclone for oil shale ash or fluidized-bed catalytic cracking (FCC) fine catalyst under similar operating conditions. The results showed that the MEIV of the cyclone for oil shale ash was 15 m/s, and for FCC fine catalyst, 23 m/s. The respective experimental MEIV values were quite different. However, the MEIV obtained from Equation (1) for oil shale ash is 9.8 m/s and for FCC fine catalyst, 10.8 m/s. The similar values are due to using the same cyclone separator and similar operating conditions, as well as due to the very similar densities of the two powder samples (the bulk density of FCC fine catalyst is 1500 kg/m³, while that of oil shale ash is 1350 kg/m³). It is also for the same reason that the MEIV values predicted from Equation (2) for oil shale ash (11.1 m/s) and FCC fine catalyst (12.3 m/s) are very similar. Both Equation (1) and Equation (2) do not provide any differences in the experimental MEIV values between oil shale ash and FCC fine catalyst. This suggests that the effect of some parameters on MEIV is ignored by these equations. This concerns primarily particle geometry, unlike particle size distribution whose effect on MEIV in our experiments was not observed.

As seen from Figure 5, the oil shale sample has a layered structure while the FCC fine catalyst sample has a spherical appearance. Two typical particles shown in Figures 5a and 5b were chosen to evaluate the sphericity (the ratio of the surface area of a sphere (with the same volume as the given particle) to the surface area of the particle). The sphericity for oil shale ash

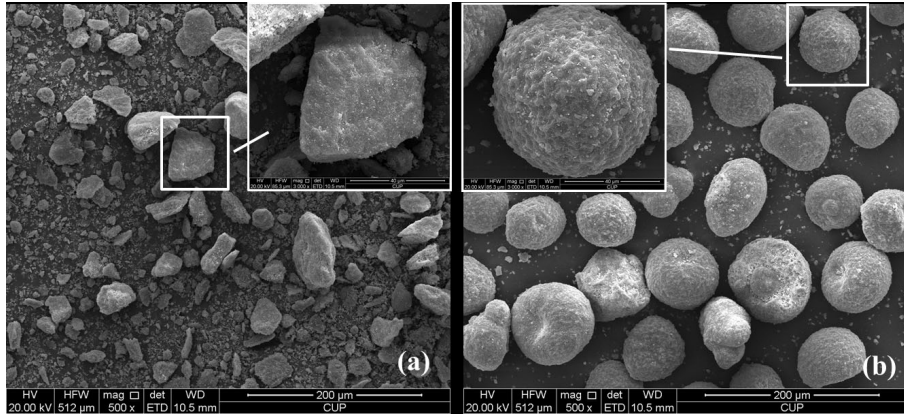


Fig. 5. Particle geometry: (a) oil shale ash, (b) FCC fine catalyst.

was 0.8 and close to 1.0 for FCC fine catalyst. The drag coefficient is closely related to particle geometry. Based on the methods of calculating the drag coefficient of spherical and non-spherical particles presented in section 4, the coefficient for oil shale ash particle (shown in Fig. 5a) is almost three times that for FCC fine catalyst particle (shown in Fig. 5b). If the two kinds of particles of the same size move with the same velocity relative to the gas, the drag force loaded on oil shale ash particle is greater than that on FCC fine catalyst particle.

The motion of a particle in a Newtonian fluid in the cyclone can be expressed by the following equation:

$$\left(\frac{\pi d_p^3}{6}\right) \rho_p \frac{d\mathbf{U}'}{dt} = \left(\frac{\pi d_p^3}{6}\right) (\rho_p - \rho_g) \mathbf{a} - C_D \left(\frac{1}{2} \rho \mathbf{U}' |\mathbf{U}'|\right) \left(\frac{\pi d_p^2}{4}\right) - \left(\frac{added}{mass}\right) - \left(\frac{Basset}{term}\right), \quad (6)$$

where \mathbf{U}' is the particle velocity vector relative to the gas; \mathbf{a} is the acceleration vector of an external force field. In the case of gas cyclones, the last two terms can be safely ignored, which means that the residual two forces – the centrifugal force acting outward and the drag force acting inward, are determinant for the motion of particles [14]. Usually, the drag force acting inward prevents separation. Combined with Stokes' Law, the terminal velocity of a particle relative to the gas during the outward radial motion can be expressed as [14]:

$$U'_r = \frac{d_p^2 \rho_p V_\theta^2}{18 \mu_g r}, \quad (7)$$

where v_θ is the tangential velocity of particle. Usually, v_θ is supposed to be similar to the tangential velocity of the gas [14–17]. Thus, $|\mathbf{U}'|$ equals U'_r if the particle's axial velocity relative to the gas is ignored. From Equation (7) it can be found that the increasing tangential velocity of the gas inside the cyclone results in the increase of the particle velocity relative to the gas. Generally, the tangential velocity of the gas increases with increasing inlet velocity. Therefore, the drag force loaded on the particle increased with the increasing inlet velocity of the cyclone, resulting in an enhanced chance of particle escape.

Besides the negative effects on gas-solid separation, the increasing inlet velocity will also result in the increase of the centrifugal force to capture more particles. The balance between these opposite effects results in the phenomenon of MEIV. Because of the significant difference in particle geometry and thus in drag coefficient between oil shale ash and FCC fine catalyst, the inlet velocity producing the balance between the above effects for oil shale ash is smaller than that for FCC fine catalyst, as observed in our experiment. Thus, the particle geometry should be an ignored parameter that affects MEIV. Unfortunately, only few studies have focused on the effect of particle geometry on the performance of the cyclone, especially on the MEIV. Therefore, it is not reasonable to include particle geometry in the proposed equation to predict MEIV. So, this effect will require further research.

4. Methods of calculating the drag coefficient

Chhabra et al. [18] presented the following expression to describe the drag coefficient of non-spherical particles:

$$C_D = \frac{24}{\text{Re}_{sph}} \left(1 + b_1 \text{Re}_{sph}^{b_2} \right) + \frac{b_3 \text{Re}_{sph}}{b_4 + \text{Re}_{sph}}. \quad (8)$$

With

$$b_1 = \exp\left(2.3288 - 6.4581\psi + 2.4486\psi^2\right), \quad (9)$$

$$b_2 = 0.0964 + 0.5565\psi, \quad (10)$$

$$b_3 = \exp\left(4.905 - 13.8944\psi + 18.4222\psi^2 - 10.2599\psi^3\right), \quad (11)$$

$$b_4 = \exp\left(1.4681 + 12.2584\psi - 20.7322\psi^2 + 15.8855\psi^3\right). \quad (12)$$

The equal volume sphere diameter (d_{sph}) was used to define the Reynolds number:

$$\text{Re}_{sph} = \frac{d_{sph} |v_p - v_g| \rho_g}{\mu_g}. \quad (13)$$

Usually, it is supposed that the particle moves with the same tangential velocity as the gas, and the particle axial velocity is ignored during analyzing its motion inside the cyclone. This allows us to replace the $|v_p - v_g|$ in Equation (13) with U_r in Equation (7).

Morsi and Alexander [19] offered the following expression to describe the drag coefficient of spherical particles:

$$C_D = \alpha_1 + \frac{\alpha_2}{\text{Re}} + \frac{\alpha_3}{\text{Re}^2}, \quad (14)$$

where α_1 , α_2 and α_3 are based on the Reynolds number (Table 3).

Table 3. The values of α_1 , α_2 and α_3 in terms of the Reynolds number

Re	α_1	α_2	α_3
$0 < \text{Re} < 0.1$	0	24	0
$0.1 < \text{Re} < 1$	3.69	22.73	0.0903
$1 < \text{Re} < 10$	1.222	29.1667	-3.8889
$10 < \text{Re} < 100$	0.6167	46.5	-116.67
$100 < \text{Re} < 1000$	0.3644	98.33	-2778
$1000 < \text{Re} < 5000$	0.357	148.62	-47500
$5000 < \text{Re} < 10000$	0.46	-490.546	578700
$\text{Re} \geq 10000$	0.5191	-1662.5	5416700

5. Conclusions

The inlet velocity has a significant effect on cyclone performances. In this work, the performance of cyclones with different sizes and geometries was investigated. The results showed the inlet area to have a significant effect on maximum efficiency inlet velocity. Maximum efficiency cross-sectional mean axial gas velocity was hardly affected by cyclone dimensions, which could be taken advantage of in designing the cyclone diameter to ensure its operation close to the maximum efficiency inlet velocity. Moreover, a significant difference between the predicted and experimental MEIV values was observed. Based on the experimental results obtained, an equation was proposed, which should allow a more precise prediction of maximum efficiency inlet velocity for oil shale ash. The difference in measured maximum efficiency inlet velocity values between oil shale ash and fluidized-bed catalytic cracking fine catalyst suggested that the particle geometry might be an ignored parameter to affect MEIV.

Acknowledgments

This work was supported by the National Natural Science Foundation of China (Grant No. 21506139), the National Key Project of Basic Research of the Ministry for Science and Technology of China (Grant

No. 2014CB744304), the Introduction of Talent Project in Taiyuan University of Technology (No. tyut-rc201478a), and the Special/Youth Foundation of Taiyuan University of Technology (No. 2014QN012), China.

Notation

a	= inlet height, m	B	= diameter of dust outlet, m
b	= inlet width, m	C_D	= drag coefficient, dimensionless
D	= diameter of cyclone, m	De	= diameter of vortex finder, m
d	= particle diameter, m	g	= acceleration of gravity, m/s^2
H	= cyclone height, m	h	= height of cylinder part, m
Q	= volumetric flow rate, m^3/s	Re	= Reynolds number, dimensionless
r	= radial coordinate, m	S	= length of vortex finder, m
v_θ	= tangential velocity, m/s		
U'_r	= radial terminal velocity of particle relative to gas, m		
KA	= ratio of cylinder cross-section to inlet cross-section, dimensionless		
v_{MEIV}	= maximum efficiency inlet velocity, m/s		
Greek letters			
ρ	= density, kg/m^3	μ	= viscosity, $Pa \cdot s$
ψ	= sphericity of particle, dimensionless		
Subscripts			
f	= first stage	g	= gas
s	= second stage	p	= particle
sph	= equal volume sphere		

REFERENCES

- Ots, A. Formation of air-polluting compounds while burning oil shale. *Oil Shale*, 1992, **9**(1), 63–75.
- Yue, C., Li, S. Combustion of oil shale particles under elevated pressures. *Oil Shale*, 2002, **19**(4), 411–417.
- Machado, N. R. C. F., Miotto, D. M. M. Synthesis of Na-A and -X zeolites from oil shale ash. *Fuel*, 2005, **84**(18), 2289–2294.
- Häsänen, H., Aunela-Tapola, L., Kinnunen, V., Larjava, K., Mehtonen, A., Salmikangas, T., Leskelä, J., Loosaar, J. Emission factors and annual emissions of bulk and trace elements from oil shale fueled power plants. *Sci. Total Environ.*, 1997, **198**(1), 1–12.
- Whitcombe, J. A., Vawter, R. G. The TOSCO-II oil shale process. In: *Science and Technology of Oil Shale* (Yen, T. E., ed.), Ann Arbor Science Publishers, Ann Arbor, Michigan, 1976, 47–64.
- Han, X., Jiang, X., Wang, H., Cui, Z. Study on design of Huadian oil shale-fired circulating fluidized bed boiler. *Fuel Process. Technol.*, 2006, **87**(4), 289–295.
- Ots, A., Pihu, T., Arro, H. Influence of sulphur dioxide and hydrogen chloride on properties of oil shale ash. *Oil Shale*, 2005, **22**(4S), 435–444.
- Wang, W. D., Zhou, C. Y. Retorting of pulverized oil shale in fluidized-bed pilot plant. *Oil Shale*, 2009, **26**(2), 108–113.

9. Wang, B. C., Liu, Y. W., Liu, J., Sun, G. G. Experimental study on separation performance of a cyclone separator for oil shale processes. *Petroleum Processing and Petrochemicals*, 2011, **42**(10), 59–62 (in Chinese).
10. Wang, W. D., Wang, Y., Ma, Q., Sun, G. G. Contrast experiments on cyclone separator performances of shale ash and FCC fine catalysts. *China Powder Science and Technology*, 2012, **18**(4), 70–72 (in Chinese).
11. Kalen, B., Zenz, F. A. Theoretical-empirical approach to saltation velocity in cyclone design. *AIChE Symp. Ser.*, 1974, **70**(137), 388–396.
12. Shi, M. X., Wu, X. L. An experimental research on the pilot-scale cold model of cyclone separator. *Chemical Engineering & Machinery*, 1993, **20**(4), 187–192 (in Chinese).
13. Shepherd, C. B., Lapple, C. E. *Air Pollution Control: A Design Approach in Cyclones*. Woveland Press, Inc., Illinois, 1939.
14. Hoffmann, A. C., Stein, L. E. *Gas Cyclones and Swirl Tubes: Principles, Design and Operation*. Springer, Berlin, Heidelberg, New York, 2007.
15. Avci, A., Karagoz, I. Effects of flow and geometrical parameters on the collection efficiency in cyclone separators. *J Aerosol Sci.*, 2003, **34**(7), 937–955.
16. Yang, J., Sun, G., Zhan, M. Prediction of maximum-efficiency inlet velocity in cyclones. *Powder Technol.*, 2015, **286**, 124–131.
17. Zhao, B. Prediction of gas-particle separation efficiency for cyclones: A time-of-flight model. *Sep. Purif. Technol.*, 2012, **85**, 171–177.
18. Chhabra, R. P., Agarwal, L., Sinha, N. K. Drag on non-spherical particles: an evaluation of available methods. *Powder Technol.*, 1999, **101**, 288–295.
19. Morsi, S. A., Alexander, A. J. An investigation of particle trajectories in two-phase flow systems. *J. Fluid Mech.*, 1972, **55**, 193–208.

Presented by J. Qian

Received April 14, 2016